

APPENDIX X

PHOTOCHEMICAL SMOG MODELLING REPORT

A REDUCTION IN FUEL REID VAPOUR PRESSURE.

**THE IMPACT ON PHOTOCHEMICAL SMOG
PRODUCTION FOR A MODELLED BRISBANE AIR
QUALITY EPISODE.**

by

Martin Cope and Josef Ischtwan

Centre for Air Quality Studies
Environment Protection Authority (Victoria)

November 1996.

EXECUTIVE SUMMARY

This report presents the results of the modelling component of the Petrol Volatility Project.

The model used for this investigation is based on the Carnegie Mellon, Caltech Institute of Technology 3-dimensional photochemical airshed model (CIT, McRae et al., 1982, Harley et al., 1993). The model describes the meteorological, physical and chemical processes of photochemical smog development from anthropogenic and biogenic photochemical smog precursors.

A South Eastern Queensland Region (SEQR) photochemical smog episode on 15 January 1987 has been the subject of previous modelling work using the CIT model. As the data sets for this event have been established within the model it has been expedient to use this model for the pilot study.

The base case, or 'status quo', model incorporated emissions for a 1993 Brisbane motor vehicle fleet for mid-week conditions using petrol with a Reid vapour pressure (RVP) of 73.5. This RVP is the same as the normal fuel used in the Brisbane fleet during summer conditions.

The estimated emissions inventory for a fuel with an RVP of 63.5 was then used in the model with all other model conditions being the same as for the base case model. The estimated emissions inventory for fuel with a RVP of 63.5 was chosen for inclusion in the model because this fuel gave the highest estimated reduction in emissions of volatile organic compounds (see table below).

Table 1

Emission test cases developed by Tilly and Wong (1996)

Test Case	Percentage change to evaporative VOC emissions	Percentage change to total motor vehicle VOC emissions	Percentage change to total daily airshed VOC emissions
RVP 73.5 kPa			
RVP 64 (63.5 kPa)	-26.4	-14.9	-9.0 ¹ (-3.4) ²
RVP 69 (68.5 kPa)	-13.8	-7.8	-4.7 (-1.8)
50% Canister replacement	-23.0	-13.0	-7.9 (-3.0)

¹assumes that motor vehicles comprise 60% of total daily anthropogenic emissions.

²assumes that motor vehicle comprise 23% of total daily anthropogenic and biogenic emissions.

To estimate the effect of changing petrol volatility the results of the base case model (RVP 73.5) have been compared to the model results obtained using the estimated emissions inventory for a RVP 63.5 fuel.

The modelling suggests that a reduction of evaporative emissions resulting from a reduction in fuel RVP to 63.5 would result in a small (2-6 percent) reduction to peak ozone concentrations. The maximum reductions were found to occur early in the development of the photochemical smog plume, where smog production is most sensitive to the concentration and reactivity of the VOC's. However, peak ozone concentrations present in the airshed later in the day (for example when the Brisbane plume impacted Surfer's Paradise), were not predicted to change significantly when the test case evaporative emissions were used.

These results suggest that for the modelled conditions, a RVP reduction or canister replacement strategy will result in small reductions only (2-6%) to the peak concentrations of photochemical smog. This reduction represents a less than proportional response if the peak ozone concentrations are assumed to develop primarily from a motor vehicle dominated anthropogenic source. The existence of a significant biogenic VOC component and the possibility that peak ozone concentrations are controlled by the availability of NO_x may be the principal factors responsible for reducing effectiveness of the VOC reduction strategies. However, it is cautioned that both of these factors are likely to be enhanced in SEQR by the presence of high ambient temperatures and solar radiation fluxes. Thus these conclusions are likely to be overly pessimistic when applied to other airsheds, or the development of photochemical smog under other classes of meteorological conditions.

TABLE OF CONTENTS

1. INTRODUCTION	1
2. AIRSHED MODELLING SYSTEM	1
3. BRISBANE PHOTOCHEMICAL SMOG BASE CASE	4
3.1. AIR QUALITY INDICATORS	4
4. FUEL VOLATILITY TEST CASES	7
5. CONCLUSIONS	9
6. REFERENCES	11
7. APPENDIX	13

LIST OF FIGURES

FIGURE 2-1	3
FIGURE 2-2	3
FIGURE 3-1	6
FIGURE 3-2	7
FIGURE 3-3	7
FIGURE 5-1	9
FIGURE 5-2	9

LIST OF TABLES

TABLE 1	7
---------	---

1. INTRODUCTION

Environment Australia commissioned The Environment Protection Authority (Victoria) to undertake the Petrol Volatility Project to investigate relationship between fuel volatility and the magnitude of evaporative losses of volatile organic compounds (VOC's) from motor vehicles. Three technical components of the study were undertaken.

- 1/ Measure the diurnal and hot soak losses of VOC's from motor vehicles for varying fuel Reid vapour pressure (RVP). This program was undertaken by the Motor Vehicle Emissions Unit, EPA(Vic) at EPA(Vic)'s Vehicle Testing Station (VTS)
- 2/ Extrapolate the results generated in 1/ to estimate changes to the evaporative emissions from a motor vehicle fleet using alternative fuel Reid vapour pressures. This component of work was undertaken by the Centre for Air Quality Studies EPA(Vic) (Tilly and Wong, 1996). Revised evaporative emissions were calculated for a 1993 Brisbane motor vehicle fleet for mid-week conditions which were suitable for the development of photochemical smog within the South Eastern Queensland Region (SEQR).
- 3/ Use a three-dimensional photochemical airshed model to determine the likely impact of the revised emissions of 2/ on the development of photochemical smog during a SEQR air quality episode.

This report presents the results of the third study component.

Section 2 of this report contains a brief introduction to the photochemical airshed modelling system used to conduct the investigation. Results from the 'base case' modelling of the SEQR photochemical smog episode are described in Section 3, and the results of a reduced fuel Reid vapour pressure 'test case' are presented in Section 4. Conclusions are given in Section 5 and a more detailed description of the model and the input data sets for the South East Queensland Region (SEQR) episode are given in the Appendix

2. AIRSHED MODELLING SYSTEM

A schematic of the airshed modelling system (AMS) is given in Figure 2-1. The system is based on the Carnegie Mellon, Caltech Institute of Technology 3-dimensional photochemical airshed model (CIT, McRae et al., 1982, Harley et al., 1993). This model describes the meteorological, physical and chemical processes of photochemical smog development from anthropogenic and biogenic photochemical smog precursors. The model has been applied extensively to the investigation of air quality problems in Los Angeles (Harley et al, and associated references), and in Australia (Cope and Happ, 1993, Cope and Ishtwan, 1995, Cope and Ishtwan, 1996, Hess, 1984).

The model requires information about the spatial and temporal variation of precursor emissions, and the spatial and temporal variation of various meteorological data including wind fields, mixing depths, ambient temperature and solar radiation fluxes. Typically the model is run for a period of one to three days, for a region which may extend up to 250 km on edge. The horizontal resolution of the model is 3 - 6 km. The vertical resolution of the model varies with height, with the greatest resolution at the surface (10-50 m), and reduced resolution at the top of the model (located at 1-3 km above ground level). Output from the model consists of instantaneous or hourly concentration predictions for a range of photochemical smog and smog precursor species (see Figure 2-1). These data may then be compared against observations, and the model evaluated, or used to compute a range of descriptive air quality metrics such as peak concentrations and population exposure.

For the SEQR modelling described herein, the meteorological data files were developed by Physick (1993) for an air quality monitoring network design study. The meteorological data are considered representative of a photochemical smog event observed on 15 January 1987. The emissions data were obtained from the 1993 SEQR emissions inventory (Morrell et al., 1995). Sources considered included motor vehicles, surface and elevated industrial, biogenic/natural and domestic and other area based sources. Motor vehicle emissions for a high oxidant (hot, elevated evaporative emissions) were used.

The modelling domain used for simulations in the (SEQR) is shown in Figure 2.2. A horizontal resolution of 3 km was used for the SEQR simulations. The model extended to 2 km in the vertical. The model was integrated for a 2-day period and results from the second day of integration are presented in the following sections. Further details regarding the configuration of the model for SEQR is contained in Appendix One, and in Ischtwan and Cope, 1996.

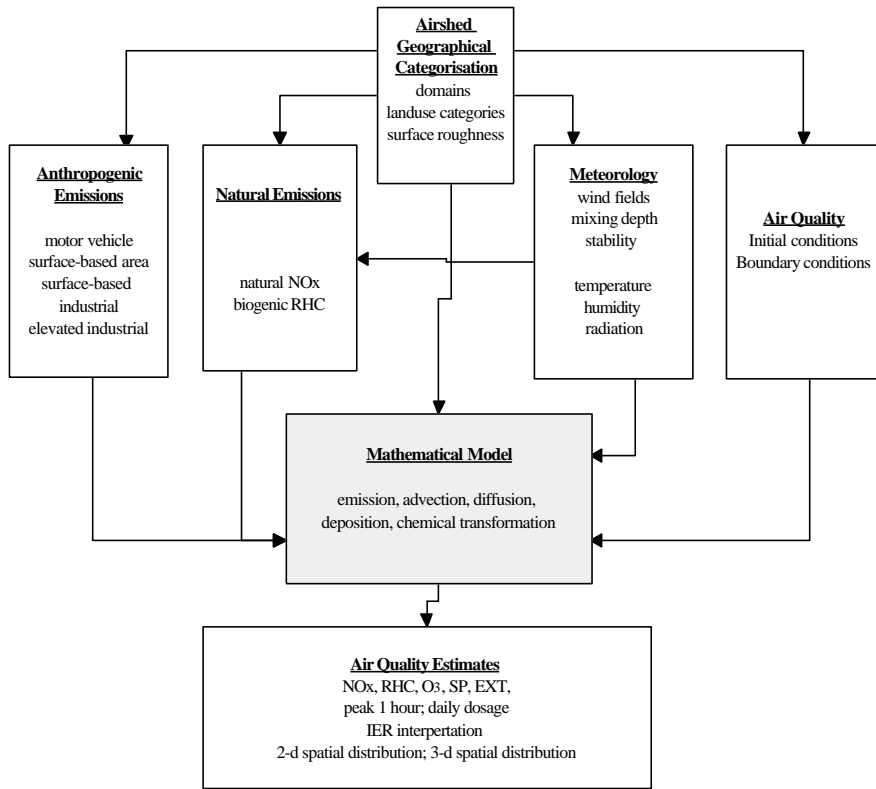


Figure 2-1
Components of the Air Quality Modelling System.

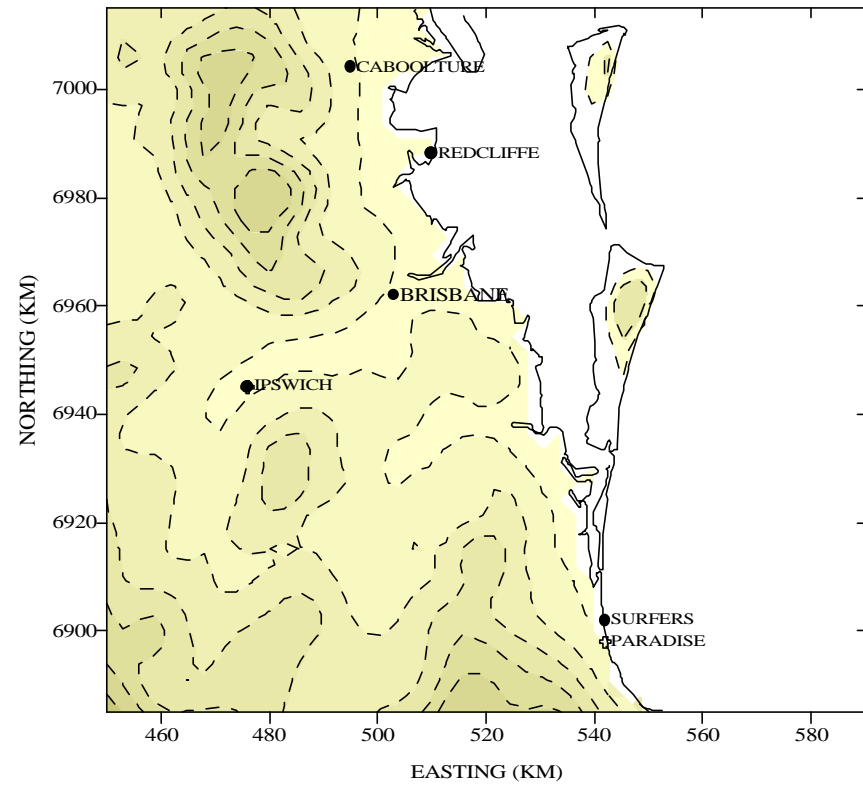


Figure 2-2
The airshed modelling domain used for the SEQR simulations

3. BRISBANE PHOTOCHEMICAL SMOG BASE CASE

In order to use the model to assess the impact of reduced motor vehicle evaporative emissions on photochemical smog levels, it is necessary to first develop a set of base case air quality predictions. Emission sensitivity studies may then be conducted by constructing test case inventories, in which selected emissions have been perturbed, generating test case air quality predictions using the airshed model, and comparing the test case predictions against the base case predictions.

Predictions of hourly averaged, ground-level concentrations of NO_y and ozone (O_3) are shown in Figure 3-1 for selected hours on 15 January 1993 of the base case simulation. A sub-set of the near surface wind vectors have also been plotted. The species NO_y is a summation of all the nitrogen species contained in the model. Thus $\text{NO}_y = \text{NO} + \text{NO}_2 + \text{secondary nitrate species}$, where NO is nitric oxide and NO_2 is nitrogen dioxide. In the current context, NO_y is merely used as a tracer for the photochemical smog precursor plume.

The development of photochemical smog is seen to have three principal stages. The first consists of the build-up of photochemical smog precursors from the high density urban regions of Brisbane and surrounding suburbs. This precursor plume is transported seawards within a westerly flow (see hour 8 and hour 10). Once over the sea, the precursor plume is predicted to be transported to the south within a northerly flow which is reinforced by the sea breeze. The second component of the photochemical smog event for this day is the development of photochemical smog within the offshore precursor plume, as it is transported southwards towards Surfer's Paradise (see hour 11). Photochemical activity within this plume is responsible for the presence of elevated concentrations of ozone (80-100 ppb), over Surfer's Paradise in the late afternoon (see hours 12-16). The third component of the event consists of the development of a photochemical smog plume from mid- to late morning Brisbane emissions. This plume, which develops in stable maritime air behind the sea breeze front, is seen to be transported inland to the south of Ipswich.

AIR QUALITY INDICATORS

A number of air quality indicators or metrics are available to summarise the air quality of a simulated air pollution episode. These range from simple indicators of maximum concentrations such as the spatial and temporal distributions of peak hourly concentration, to estimates of exposure such as the spatial distribution of peak daily dosage or peak population-weighted daily dosage. In the case of photochemical smog, these metrics may be calculated for ozone alone, or for a sum of ozone and a range of additional secondary oxidant products (such as nitrogen dioxide, nitric acid, peroxyacetylnitrate and particulate nitrate). For the purposes of the current study, the consideration of air quality metrics has been restricted to the diurnal and spatial distribution of peak one-hour ozone. The interested reader is referred to Ischtwan and Cope (1996) for the presentation of additional air quality metrics.

The predicted diurnal distribution of peak one-hour ozone concentration is shown in Figure 3-2. This plot was developed by searching the hourly predictions of ground-level ozone for the maximum concentration. It should be noted that the position of the hourly ozone peak will most likely change each hour. Figure 3-2 shows that the peak hourly concentrations decreased from about 55 ppb at hour 1 to a low of about 35 ppb at hour 7. The high initial concentrations of ozone (background levels are typically 25-35 ppb) are the result of photochemical production on the previous day of the simulation. Concentrations have decreased during nocturnal hours because ozone is depleted at the surface through the process of dry deposition. Strong radiation and high temperatures after hour 8 contribute to a rapid rate of ozone production, resulting in the development of a 115 ppb ozone peak by hour 10. This initial peak, which is sited close to the mouth of the Brisbane River, is considered to be generated by a combination of urban (primarily motor vehicle) and industrial emissions. The peak is predicted to last for only one hour before dilution processes lead to a rapid reduction of ozone concentration to less than 80 ppb. The second ozone peak is generated within the urban plume as it is advected southward down the coast (see Figure 3-1). A peak ozone concentration of 110 ppb is reached at hour 13. After this time, peak ozone concentrations plateau for approximately 3 hours before decreasing. A source sensitivity study (Ischtwan and Cope 1996) has demonstrated that ozone production between hours 8

and 13 is most sensitive to the magnitude and reactivity of VOC emissions. After hour 13, peak ozone concentrations become sensitive to the magnitude of NO_x emissions.

The spatial distribution of peak one-hour ozone concentration is shown in Figure 3-3. The spatial distribution is generated by scanning the grids of hourly ozone predictions for the maximum predicted ozone concentration at each grid point. It can be seen that peak one hour ozone concentrations are predicted to exceed 80 ppb for a region which extends from Brisbane to south of Surfer's Paradise, and inland to the west of Ipswich. The highest concentrations are predicted to occur over a region which extends along the coast towards Surfer's Paradise. This region corresponds to the development of photochemical smog from morning peak hour Brisbane emissions (see Figure 3-1). A second region of elevated ozone concentrations are located inland and to the south of Brisbane. These concentrations were generated from late morning precursor emissions which were advected inland within the sea breeze. The hour 9 ozone peak displayed in Figure 3.2 can be seen just to the south of the Brisbane River mouth.

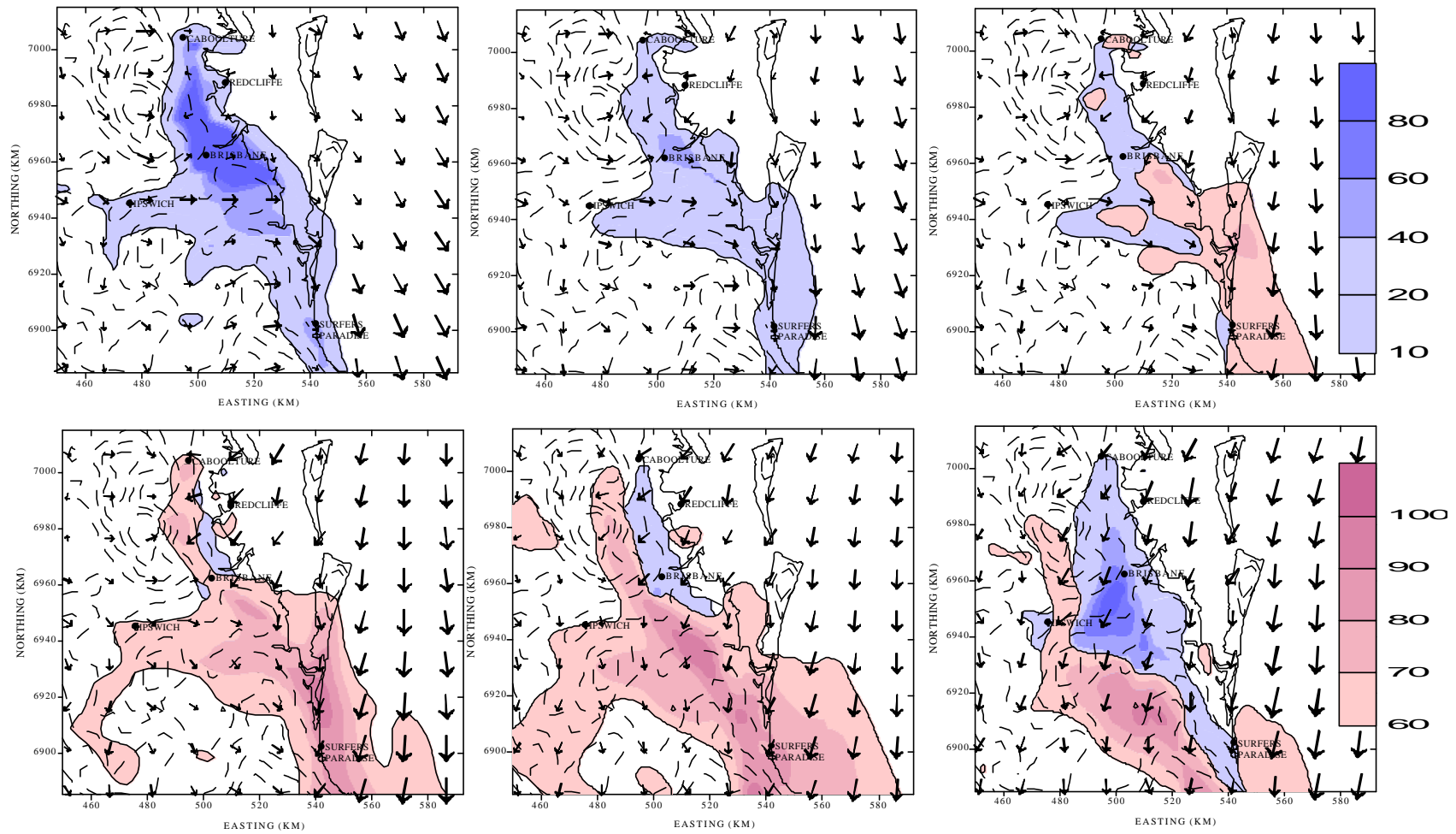


Figure 3-1
The predicted spatial distribution of ground level NO_y , O_3 and horizontal wind for (top) hour 8, 10, 12 and (bottom) hour 14, 16, 18.

Error! Not a valid link.

Figure 3-2

The predicted diurnal variation of maximum, one-hour ground level ozone concentration for the base case.

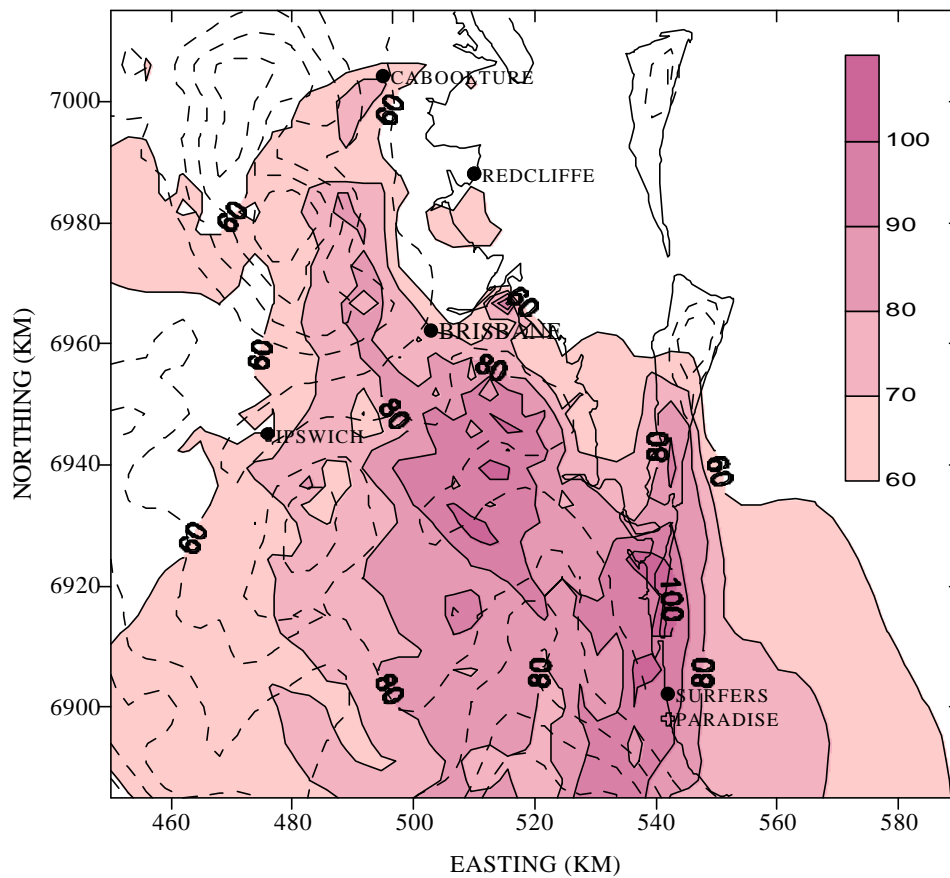


Figure 3-3

The predicted spatial distribution of maximum, one-hour ground level ozone concentration for the base case.

4. FUEL VOLATILITY TEST CASES

Now that the base case air quality metrics have been determined, the model may be used to assess the changes which result when the base case emissions are varied. Three different emission test cases have been established to investigate the changes to photochemical smog development resulting from evaporative emissions reductions which are caused by a variation of fuel Reid vapour pressure, or by canister replacement (Tilly and Wong, 1996).

Table 2

Emission test cases developed by Tilly and Wong (1996)

Test Case	Percentage change to evaporative VOC emissions	Percentage change to total motor vehicle VOC emissions	Percentage change to total daily airshed VOC emissions
RVP 73.5 kPa			
RVP 64 (63.5 kPa)	-26.4	-14.9	-9.0 ¹ (-3.4) ²
RVP 69 (68.5 kPa)	-13.8	-7.8	-4.7 (-1.8)
50% Canister replacement	-23.0	-13.0	-7.9 (-3.0)

¹assumes that motor vehicles comprise 60% of total daily anthropogenic emissions.

²assumes that motor vehicle comprise 23% of total daily anthropogenic and biogenic emissions.

It can be seen from Table 2 that a reduction of the fuel Reid vapour pressure from 73.5 to 63.5 kPa is predicted to result in a 26 percent reduction of evaporative VOC emissions from a SEQR vehicle fleet, for ambient conditions typical of a SEQR high oxidant day. This is equivalent to a 15 percent reduction of the total (evaporative+tailpipe) VOC emissions from the vehicle fleet and a nine percent reduction of the total daily anthropogenic VOC emissions from SEQR. The latter is reduced to 3.4 percent when the contribution of biogenic VOC's are also included in the total. A Reid vapour pressure reduction of one-half the previous case is calculated to result in VOC emissions reductions which are also about one-half of the reductions given for the previous case. The test case scenario in which 50% of carbon canisters are replaced in the motor vehicle fleet is estimated to result in VOC emission reductions that have a less significant impact than those calculated for the RVP-64 test case scenario.

Modelling results are presented below for the RVP 64 test case only. This has been done because a previous study (Ischtwan and Cope 1996) suggested that peak concentrations of photochemical smog will decrease monotonically (but not necessarily proportionately) with a reduction in ROC emissions from motor vehicles. The RVP 64 test case has the maximum ROC reduction of the three test cases considered in this study (see Table 2). Thus the degree of ozone change resulting from the RVP-64 test case may be considered to represent an upper bound for the three considered cases.

The variation in the diurnal and spatial distributions of peak one-hour ozone concentration respectively are presented in Figure 4-1 and Figure 4-2 for the RVP-64 test case. In Figure 4.1 it can be seen that maximum base case diurnal ozone concentrations are generally reduced by 2-6 ppb. The greatest reduction is predicted to occur at hour 10, which corresponds to the time of occurrence of the photochemical smog peak to the south of the Brisbane river mouth. A small increase in ozone, which is predicted to occur for the hour prior to this time, probably results from inaccuracies in the numerical chemical solver during the period of rapid ozone production between hour 8 and 10. The magnitude of this peak may be considered to be indicative of the noise level in the model at this time. After hour 10, the model predicts that the RVP-64 test case will result in reductions of 2-3 ppb (2-3 percent) compared to the maximum predicted base case ozone concentrations. These reductions represent a less than proportional reduction compared to the modelled VOC reductions if it is assumed that the peak ozone concentrations result primarily from a motor vehicle dominated anthropogenic source. In this case, such a reduced sensitivity may result from the fact that peak photochemical smog production within SEQR is increasingly controlled by the availability of NO_x as the day proceeds and NO_x within the urban plume is progressively converted to stable nitrate compounds (see Ischtwan and Cope 1996). However, the high levels of biogenic VOC projected for the Brisbane region (Morrell et al., 1995) may also lead to a reduced sensitivity of smog production to anthropogenic VOC emissions.

The spatial distribution of peak one-hour ozone concentration differences (TEST-BASE) are shown in Figure 4-2. It can be seen that the areas of maximum reduction (4-6 ppb) occur over the eastern Brisbane region. As noted above, these reductions are predicted to occur at the time of the morning photochemical smog peak and correspond to a period when photochemical smog production is most sensitive to the concentration and reactivity of ROC. On the other hand, peak ozone concentrations over, and to the north of, Surfer's Paradise are predicted to be reduced by only 2-3 ppb. Again, this is probably due to the fact that the photochemical plume is considerably aged by this time, and photochemical production has become limited by the availability of NO_x .

Error! Not a valid link.

Figure 4-1

The predicted diurnal variation of peak one-hour ozone concentration and concentration change (TEST-BASE) for the test case (RVP-64) and base case.

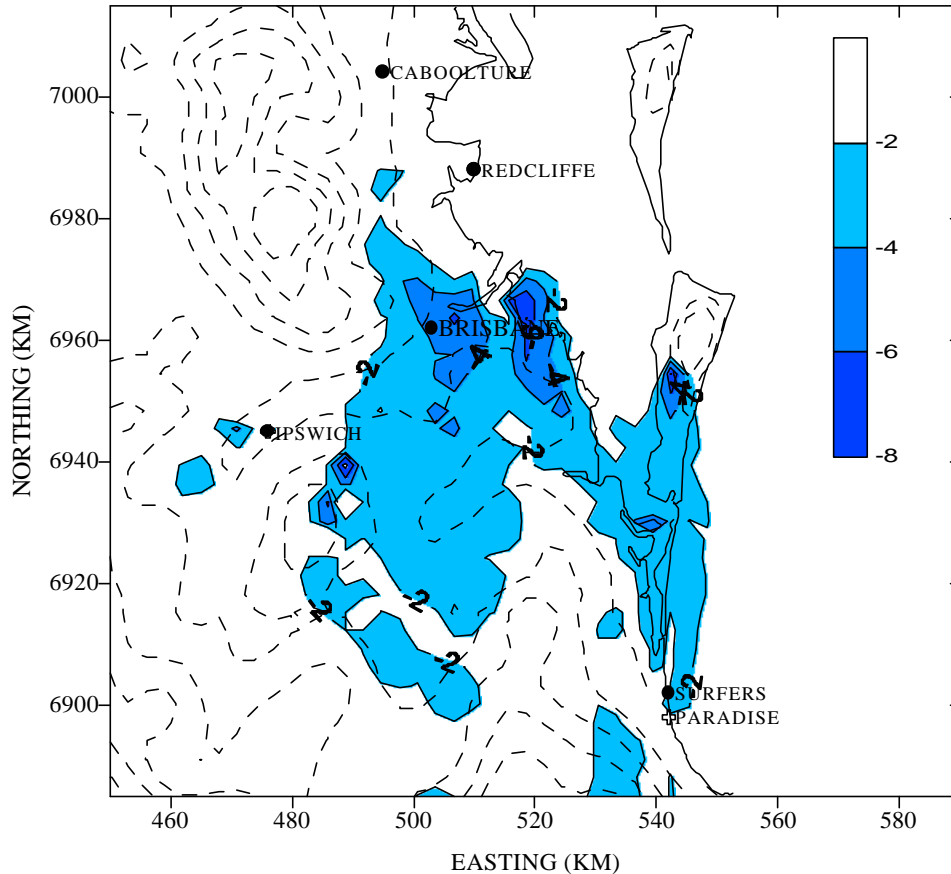


Figure 4-2

The spatial distribution of peak one-hour ozone concentration change (ppb) for the RVP-64 test case and the base case (changes are calculated as TEST-BASE).

5. CONCLUSIONS

A 3-dimensional photochemical airshed model has been used to investigate the impact of reduced evaporative emissions on photochemical smog development during a SEQR air quality episode. The reduced levels of evaporative emissions used in the modelling result from a reduction in the volatility of petrol.

The case in question consisted of a SEQR photochemical smog episode, which has already been the subject of a preliminary modelling study (Ischtwan and Cope 1996). Motor vehicle emissions were considered to be representative of a 1993 fleet, operating under ambient conditions suitable for the generation of enhanced levels of evaporative emissions. A 1993 base case was established in which the petrol-fuelled component of the motor vehicle fleet was assumed to operate on petrol with an RVP of 73.5 (the normal RVP of fuel used in the Brisbane fleet during summer conditions). Peak ozone concentrations were predicted to exceed 0.1 ppm and a plume of elevated ozone concentrations was predicted to extend from Brisbane to Surfers' Paradise on the coast, and inland to the south of Ipswich.

Three test cases of reduced evaporative emissions from motor vehicles were considered. In the first, a petrol RVP of 63.5 was assumed, resulting in a 15% reduction of VOC emissions from the motor vehicle fleet and a 3-9% reduction of the total daily SEQR VOC emissions. A petrol RVP of 68.5 was

assumed for the second case, resulting in a 8% reduction of VOC emissions from the motor vehicle fleet (2-5% reduction of total daily SEQR emissions). The final test case assumed that 50% of the motor vehicle fleet were fitted with fresh activated carbon canisters, resulting in a 13% reduction of VOC emissions from the motor vehicle fleet (3-8% of total daily SEQR VOC emissions).

Model results from the first test case only were compared with base case predictions. This was done because the considered case is most likely to provide the maximum reductions in photochemical smog production compared to the other test cases. The modelling suggested that a reduction of evaporative emissions of the magnitude considered here would result in only small reductions peak ozone concentrations of 2-6 percent. The maximum reduction was found to occur early in the development of the photochemical smog plume, where smog production is most sensitive to the concentration and reactivity of the VOC's. Peak ozone concentrations present in the airshed later in the day (for example, when the Brisbane plume impacted Surfer's Paradise) were not predicted to change significantly when the RVP 63.5 test case evaporative emissions were used.

These results suggest that, for the modelled conditions, a RVP reduction or canister replacement strategy will result in a reduction in peak concentrations of photochemical smog of 2-6%. This reduction represents a less than proportional response if the peak ozone concentrations are assumed to develop primarily from a motor vehicle dominated anthropogenic source. The existence of a significant biogenic VOC component and the possibility that peak ozone concentrations are controlled by the availability of NO_x may be the principal factors responsible for reducing the effectiveness of the VOC reduction strategies. However, the influence of the biogenic VOCs and the availability of NO_x are likely to be exaggerated in the in SEQR because of the presence of high ambient temperatures and solar radiation fluxes. Thus these conclusions are likely to be overly pessimistic when applied to other airsheds, or to the development of photochemical smog under other classes of meteorological conditions.

6. REFERENCES

- Azzi, M., Johnson, G., and Cope, M.E. (1992), *An Introduction To The Generic Reaction Set Photochemical Mechanism*, in: Proceedings of the 11th International Conference of the Clean Air Society of Australia and New Zealand (Brisbane).
- Briggs G. A. (1975). *Plume Rise Predictions*. In Lectures on Air Pollution and Environmental Impact Analysis pp.59-11 (ed. D. A. Haugen) (American Meteorological Society: Boston).
- Caughey S. J., Wyngaard J.C., and Kaimal J.C. (1979). *J. Atmos. Sci.*, **36** 1041-1052.
- Carnovale, F., Tilly, K., Stuart, A., Carvalho, C., Summers, M., and Eriksen, P. (1994), *Metropolitan Air Quality Study - Air Emissions Inventory* (EPAV, Melbourne), in: MAQS (Coffey Partners, Sydney).
- Cope M. and Happ C., 1993. *Ozone goal preliminary compliance projections for 2005*. Final Report to NHMRC.
- Cope M. E., and Ischtwan J. (1995), *MAQS Final Report*. Report to NSW Environmental Protection Authority, Task 4: Airshed modelling.
- Cope M. E., and Ischtwan J. (1996), *PPSS Final Report*. Report to Western Power and WA Environmental Protection Authority, Photochemical Airshed modelling.
- Deardorff, J. W., and Willis, G. E. (1975). *Appl. Meteorol.* **14**, 1451-1458.
- Dodge M.C. 1989, *Journal of Geophysical Research*, **94**, (4) 5121-5135.
- Environment Protection Authority of Victoria (1985), *The Impact of Emissions from Newport D Power Station on Air Quality*. Melbourne, Victoria
- Gear C.W. (1971), *Numerical Initial Value Problems in Ordinary Differential Equations*. Prentice-Hall, Englewood Cliffs, NJ.
- Gery M. W., Whitten G. Z., Killus J. P. and Dodge M. (1989). *Journal of Geophysical Research*, **94** (10) 12925-12956.
- Harley R. A., Russell A. G., McRae G. J., Cass G. R., and Seinfeld J. H. (1993), *Environ. Sci. Technol.*, **27**, 378-388.
- Hess G. D. (1984). *Photochemical Model Assessment of Air Quality*. in Proc. Eighth Internat. Clean Air Conf., Melbourne, 6-11 May 1984. The Clean Air Society of Australia and New Zealand.
- Holtslag and Boville (1993), *Journal of Climate*, **6**, 1825-1842.
- James B. (1994), *Perth Photochemical Smog Study Motor Vehicle Emissions Inventory* (Department of Transport Report 358, Nedlands WA 6009).

Johnson, G. M (1991), *Explanatory Notes and Supplementary Materials*, bound papers and reports for seminar at U.S.EPA, Research Triangle Park, N. C., 12-13 December.

Lurmann F. W., Carter W. P. L., and Coyner L. A. (1987), *A surrogate species chemical reaction mechanism for urban-scale air quality simulation models, Vol. I- Adaptation of the mechanism* (U.S. Environmental Protection Agency, NC 27711)

McRae G. J., Goodin W. R. , and Seinfeld J. H. (1982), *Mathematical Modeling of Photochemical Air Pollution* (California Institute of Technology, Pasadena, California).

McRae, G.J., Russell, A.G., and Harley, R.A. (1992), *CIT Photochemical Airshed Model - Users Manual* (Carnegie Mellon University, Pittsburgh, PA, and California Institute of Technology, Pasadena, CA).

Milford, J.B, Russell, A.G., and McRae, G.J. (1989), *Environ. Sci. Technol.* **23**, 1290-1301.

Morrell A., Stuart A., Tope H. (1995). *South East Queensland Air Emissions Inventory*. Draft Final Report to Queensland Department of Environment.

Morris R.E. and Myers T.C., 1990. *Users Guide for the Urban Airshed Model: Volume I*. EPA Research Triangle Park, N.C. USA (pub. EPA-450/4-90-007A).

Physick, W.L., (1993), *Windfield modelling of two case study days using LADM for the purposes of network design*. 106pp. In: Brisbane Windfield Study. Coffey Partners International. Final Report to QLD. Department of Environment and Heritage. April 1993.

Scheffe R. D., and Morris R. E. (1993), *Atm. Environ.*, **27B**, 23-39.

Streeton J.A. (1990), *Air Pollution Health Effects And Air Quality Objectives In Victoria* (EPAV, Melbourne).

Tilly K., and Wong N., (1996), *Fuel Reid Vapour Pressure Reductions and Canister Replacement Inventory Modelling of the Brisbane Region*. (EPAV Melbourne), Submission to the Petrol Volatility Project, Federal Office of Road Safety, in press.

APPENDIX

A DATA AND DATA PROCESSING

In order to simulate an oxidant event in detail, the airshed model requires input from nineteen data files per day of simulation. The files provide descriptions of the modelling region, the temporal and spatial distribution of precursor emissions, initial and inflow contaminant concentrations, vector wind fields, mixing depths, temperature, radiation fluxes and surface type.

In Table A.1 are described the major data sets, which must be assembled, together with the methods of construction used for the SEQR simulations.

A.1 Land use and surface roughness definition files

The photochemical airshed model requires that each cell be assigned a urban/rural/ocean land-use definition, a fractional land use class for up to 32 land-use categories and a grid-averaged surface roughness. These definitions are required for the specification of hydrocarbon splits used for assigning organic classes from non-methane-hydrocarbon (NMHC) measurements, the surface deposition resistance for each chemical species, and surface roughness for eddy diffusivity calculations.

For preliminary SEQR simulations we have merely defined the land-use category of all cells within the master grid to be either of type rural or ocean. Moreover, the rural land use category has been given a surface roughness and a surface uptake resistance appropriate for a mixed-forest category (see McRae et al. (1992) for further details). The use of the 2 categories described above will enable the important distinction to be made between transport over water (with small depositional losses for insoluble species such as ozone), and transport over land. Numerical simulations have demonstrated that, provided the land/sea demarcation has been made, the use of a relatively crude land use categorisation does not significantly change the location and timing of peak photochemical smog concentrations. More recently, we have attempted to make more subtle distinctions on the basis of varying vegetation types and urban/rural division.

The land sea mapping required for the determination of these categories was determined by interpolating land/sea fraction data provided in LADM output files.

A.2 Meteorological data sets

A.2.1 Vector wind fields

The CIT photochemical airshed model performs 3-dimensional advection calculations using divergence-free layer-averaged vector wind fields. These fields are developed from CSIRO DAR's Lagrangian Atmospheric Dispersion Model (LADM, Physick. (1993)) estimates using a multi-stage process.

1/ Horizontal vector wind fields from the LADM 5 km and 2.5 km grids (50x50x20 levels) are interpolated onto the MDSG.

2/ The 20 levels of interpolated winds are averaged over the 10 levels used within the airshed model and the resultant wind fields are (optionally) smoothed.

3/ With the exception of the upper boundary, vertical velocities are calculated subject to the constraint that the 3-dimensional wind field is mass consistent. The vertical velocity on the upper boundary is set to zero in order to maintain a zero flux boundary condition.

4/ Anomalous divergence in the upper layer of the model, introduced through the application of the zero flux boundary condition, is removed from the entire grid using an iterative divergence minimisation scheme.

We have found that this procedure best reproduces the properties of the LADM fields during the coordinate mapping step. Examples of the resultant wind field for level 1 (0-25 meters) and level 4 (250-349 meters) for hours 0700 and 1300 on 150187 are shown in Fig. A.2. This field shows two of the crucial mesoscale flows responsible for photochemical smog development in the SEQR region. First, The model predicts stable flow conditions with strong vertical shear in the morning. Note that in the morning of the modelled event, wind changes direction and speed with height (Figs. A.1a-b). The boundary layer is estimated to be not well mixed in the morning of this event. Second, the sea breeze is estimated to develop around hour 1300. Figure A.2c indicates for layer 1 the arrival of the sea breeze at the coast at around hour 1300. As it will be shown below, the mixed layer depth has developed at this time to a maximum height of approximately 800 meters at the coast. The sea breeze (Fig. A.2c) is estimated to undercut airmass at altitudes below 500 meters (Fig. A.1d).

Table A.1
List of data sets required by the photochemical airshed model

DATA FILE DESCRIPTION	PURPOSE	METHOD OF CONSTRUCTION
GEOGRAPHICAL		
Master Data Storage Grid Land use, surface roughness and surface resistance	Storage region for all data files Used in the definition of initial conditions. Also used to prescribe surface resistance for deposition calculations and eddy diffusivity	Based on trajectory analysis and modelling requirements Land/ocean demarcation only
METEOROLOGY		
Mixing depth fields	Used to determine vertical eddy diffusivity profiles	Derive from LADM estimates of σ_u/σ_z ; σ_q/σ_z .
Three dimensional wind fields	Used for advection calculations	Derive from LADM wind field estimates
Obukhov parameters	Used in eddy diffusivity and deposition calculations	Derive from LADM estimates of u_* and q_* .
Surface temperature field	Used to calculate temperature dependant chemical reaction rates	Derive from temperature observations
Absolute humidity fields	Used for chemical reaction calculations	Derive from humidity observations
Solar radiation scaling fields	Used to determine radiation dependant surface resistances	Derive from radiation observations, or assume clear skies
UV radiation scaling fields	Used to calculate photolytic reaction rates	Derive from radiation observations, or assume clear skies
EMISSIONS		
Area source emissions	Use to define urban and biogenic emission fluxes	SEQR emissions inventory averaged to grid resolution. Biogenics estimated by assuming land areas covered by mixed forest.
Elevated point source emissions	Use to define large industrial emissions	SEQR emissions inventory averaged to grid resolution.
AIR QUALITY		
Initial concentrations	Used to define the initial state of air quality within the region	Set to background levels observed in Latrobe Valley, Victoria and model pre-event day.
Boundary concentrations	Used to define the air quality on the boundaries of the model	Set to background levels observed in Latrobe Valley, Victoria and properly define computational region to reduce sensitivity to boundary conditions

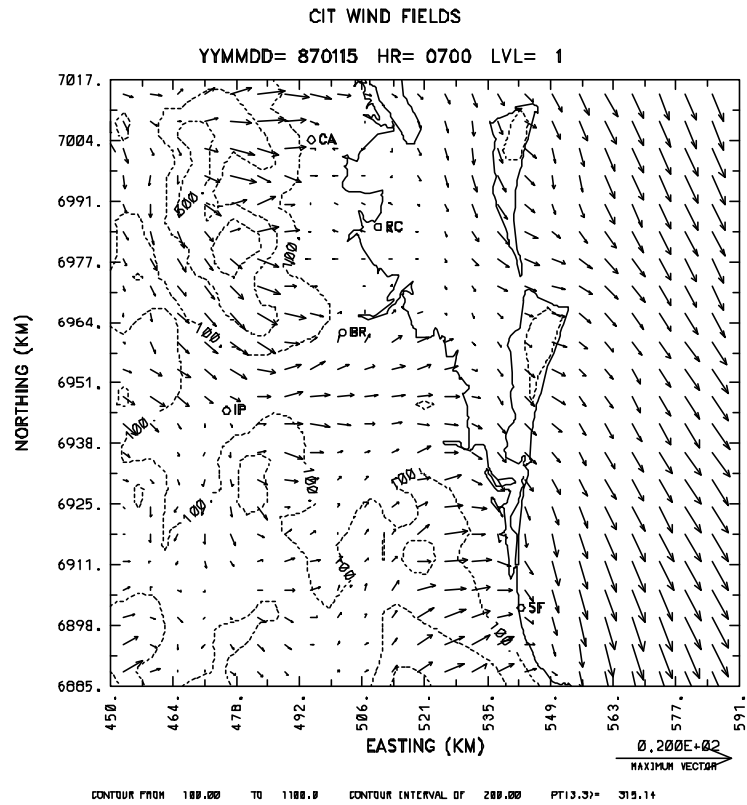


Figure A.1a
Estimated wind field for layer 1 (0-24 m) at hour 0700, 15 January 1987.

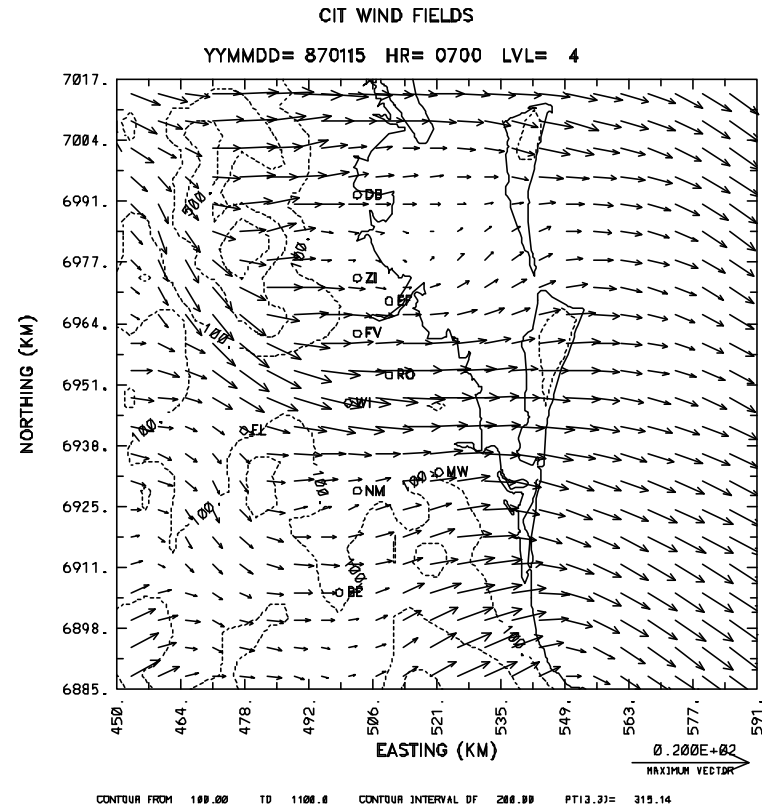


Figure A.1(b)
Estimated wind field for layer 4 (250-349 m) at hour 0700, 15 January 1987.

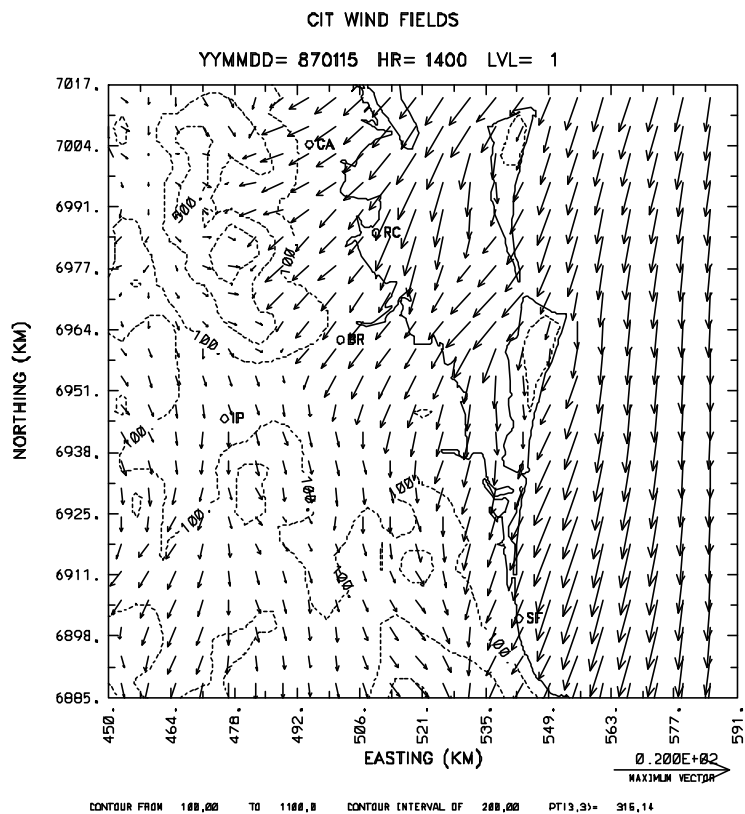


Figure A.1c
Estimated wind field for layer 1 (0-24 m) at hour 1300, 15 January 1987.

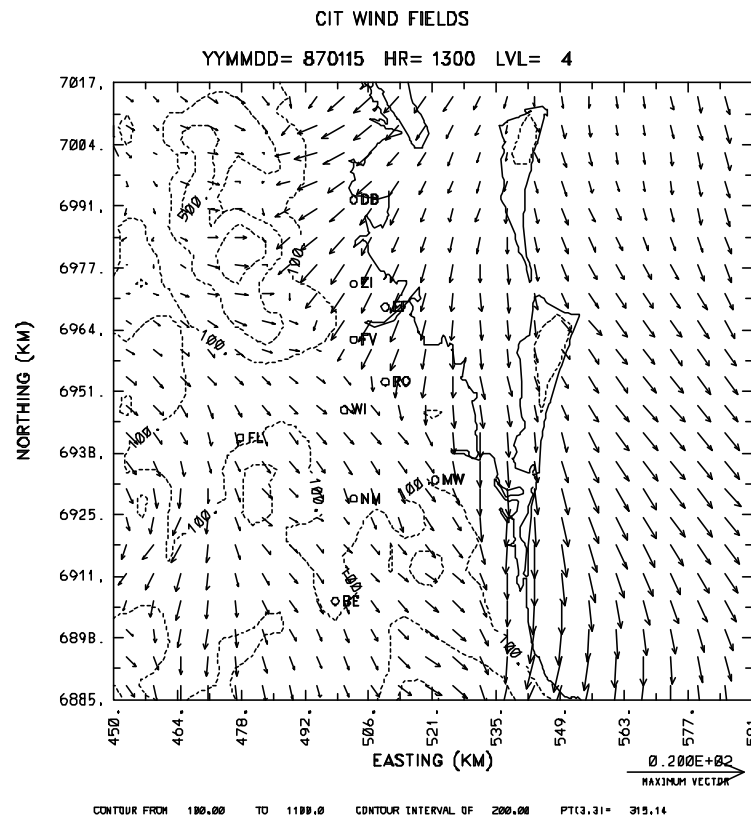


Figure A.1d
Estimated wind field for layer 4 (250-349 m) at hour 1300, 15 January 1987.

A.2.2 Mixing depths

The proper prescription of the spatial and temporal variation in mixing depth is a crucial aspect of photochemical airshed modelling, because the mixing depth determines both the degree of dilution (and hence the rate of chemical reaction), and the mean transport direction (defined by the layer averaged wind direction). Mixing depths for stable and unstable conditions have been derived from the estimated vertical profiles of wind speed and potential temperature using a gradient Richardson number scheme (Holtslag and Boville (1993)). This scheme is optionally supplemented by an additional search for a thermal internal boundary layer (TIBL) during sea breeze conditions. For the current study we define the TIBL as the height at which the potential temperature gradient exceeds 1 K/km.

Estimated mixing depths are shown for two sites in the SEQ region for the 15 January 1987 simulation in Fig. A.3. In the morning between hours 0700 and 1100 the mixing depth rises from 30 m to above 400 m and decreases between hours 1400 and 1600 due to the arrival of the sea breeze at these locations. Figure A.4 displays the spatial variation of the mixing depth fields at hours 0900 and 1400.

A.2.3 Surface temperature

Ambient temperature is required by the airshed model for the determination of temperature dependant photochemical reaction rates. For the current study, gridded temperature fields were derived from near-surface temperature observations made at the following stations: Amberley, Archerfield, Brisbane Airport, Caloundra, Cape Moreton, Gatton, Ipswich, Mt Glorious, Nambour, Samford and Southport. For example, shown in Fig. A.4 are hourly temperature observations at Brisbane Airport for 15 January 1987. It can be seen that temperatures of 25 C were observed overnight before rising rapidly to 35 C by hour 1200. High concentrations of photochemical smog are typically associated with ambient temperatures in excess of 30 C. With the exception of a first order correction for height (assuming an adiabatic rate of cooling) observations were applied to the entire MDSG without further modification.

A.2.4 Absolute Humidity

Absolute humidity have been calculated from dewpoint temperatures and atmospheric pressures using the Clausius-Clapeyron equation. The data for dewpoint temperatures and atmospheric pressures are available from the observations stations data mentioned in Section A.1.3. for the construction of spatial and temporal gridded fields the same interpolation procedures have been employed as for the temperature fields.

A.2.5 Solar and UV radiation scaling fields

The model uses a look-up table of actinic fluxes (given as a function of zenith angle) to determine the rate coefficients for a number of important photolytic reactions. The actinic fluxes have been calculated using a theoretical model representative of clean air conditions in Southern California. In order to correctly represent other regions of the world, and/or cloudy or hazy conditions, gridded, hourly radiation scale factors may be input into the model. These scale factors are derived by comparing observed and theoretical values of total solar radiation (TSR) or ultra-violet radiation (UV). For the SEQR monitoring study, we have either assumed clear sky conditions.

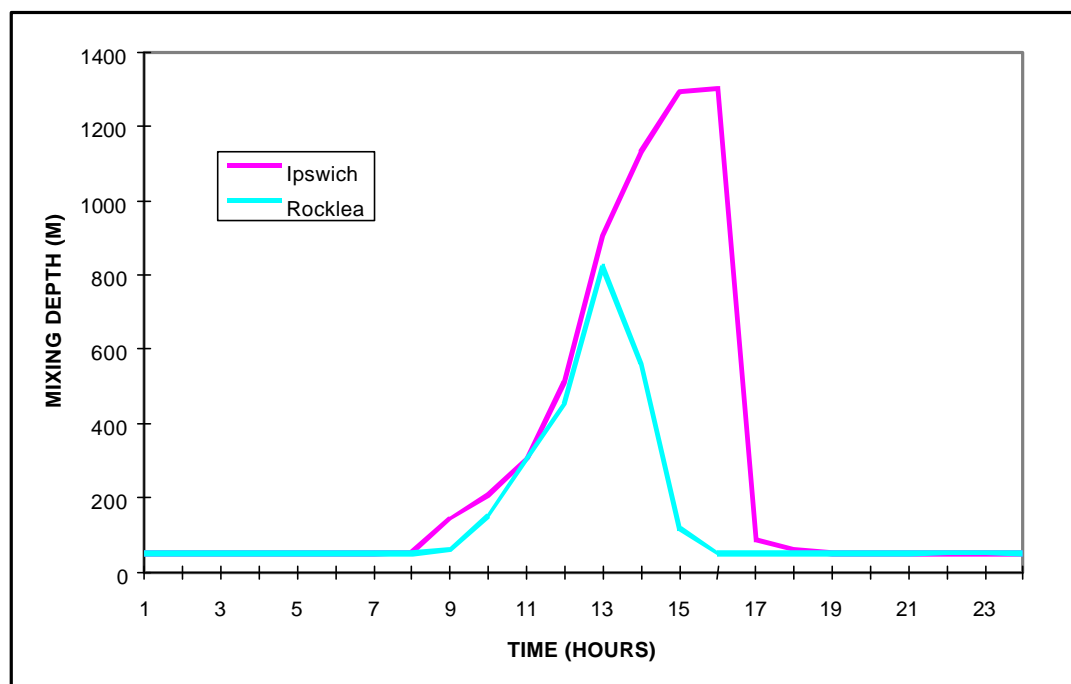


Figure A.2
CIT model mixing depth at Rocklea and Ipswich.

A.3 Initial and boundary species concentrations

The model requires the specification of both initial and boundary inflow contaminant concentrations. Boundary conditions for the top of the computational domain need not be specified because the model has a no-flux boundary condition on this surface.

We have defined the initial and boundary concentrations to be representative of the background levels observed in and around Melbourne and Latrobe Valley (Table A.5). However, we have also attempted to minimise the sensitivity of smog predictions to reasonable errors in the prescription of the initial and boundary conditions by an appropriate selection of both computation domain size and integration period.

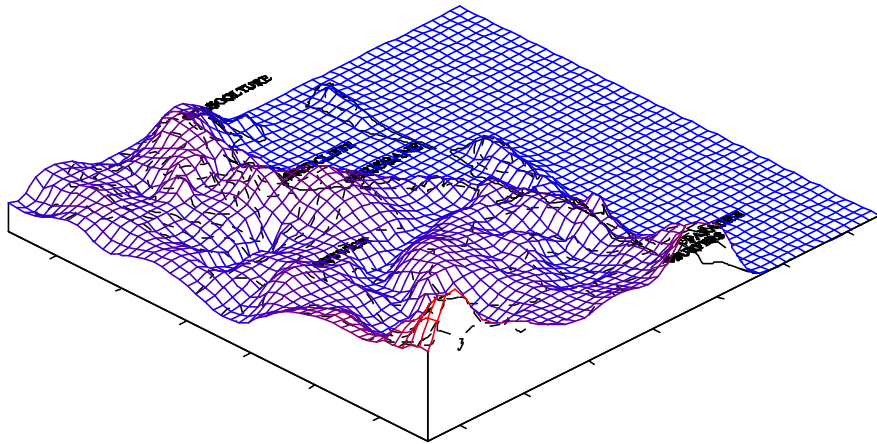


Figure A3.(a)
Schematic representation of mixing depth field at hour 0900, 15 January 1987.
(Minimum of mixing depth: 50 m; maximum of mixing depth: 705 m.)

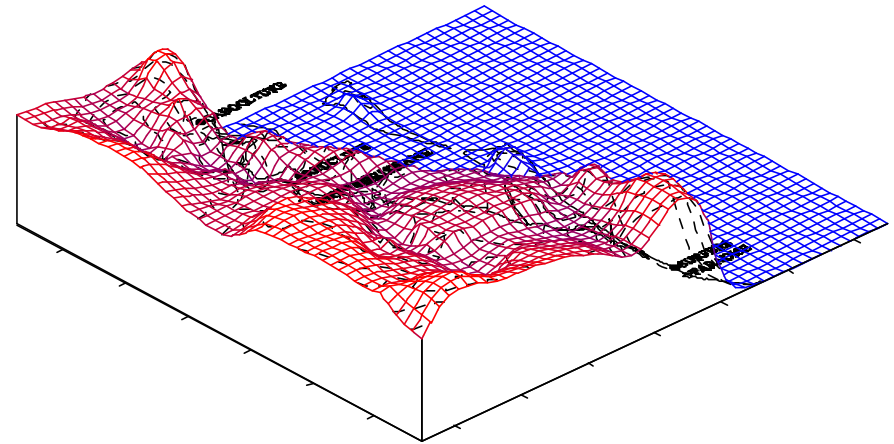


Figure A.3(b)
Schematic representation of mixing depth field at hour 1300, 15 January 1987.
(Minimum of mixing depth: 50 m; maximum of mixing depth: 1485.)

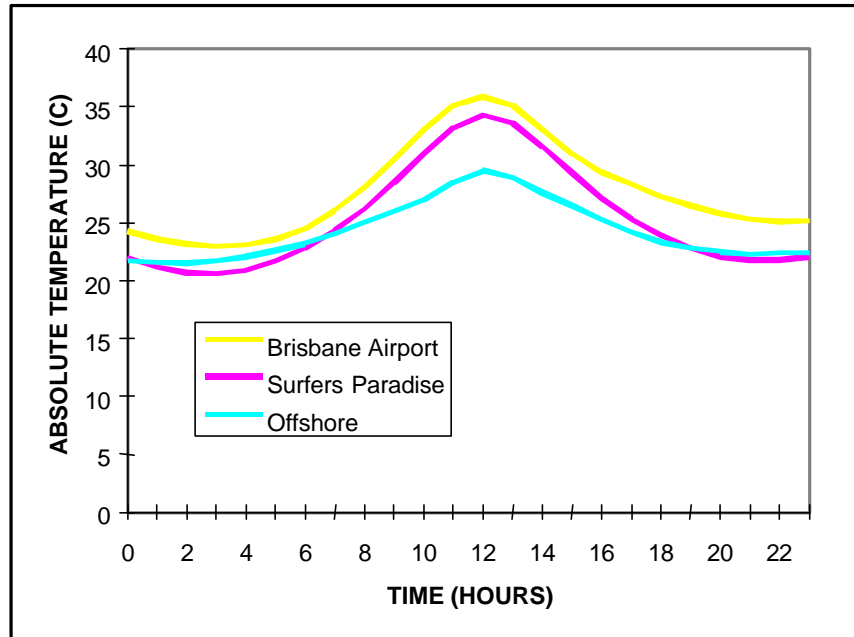


Figure A.4(a)
Diurnal profiles of estimated absolute temperatures at Brisbane Airport, Surfers Paradise and a location offshore for 15 January 1987.

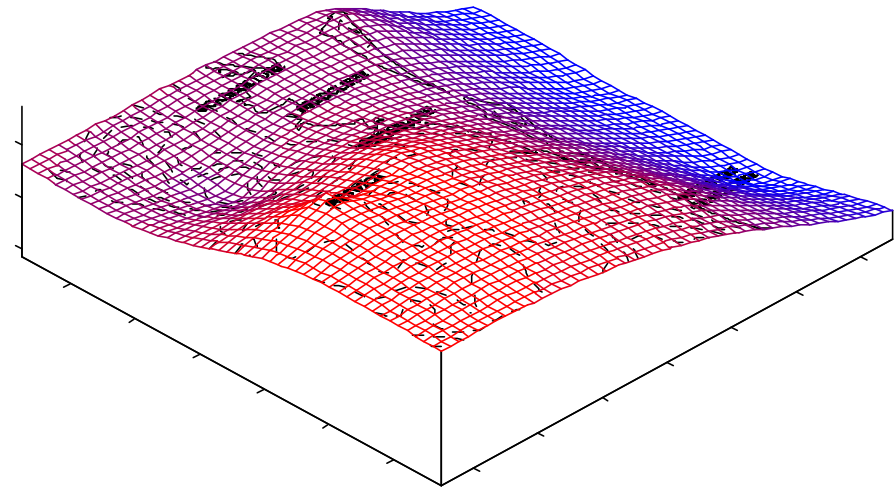


Figure A.4(b)
Schematic representation of absolute temperature field at hour 1300, 15 January 1987. (Minimum temperature: 23 C; maximum temperature: 37 C)

Table A.2
Initial And Boundary Concentrations of the Modelled Contaminant Species

Species	Near surface concentration	Upper level concentration
NO	0.5 ppb	0.5 ppb
NO ₂	0.05 ppb	0.05 ppb
O ₃	25 ppb	25 ppb
CO	200 ppb	200 ppb
SO ₂	0.1 ppb	0.1 ppb
RHC	15 ppbC	5 ppbC
HCHO	2 ppb	1 ppb
higher aldehydes	0.5 ppb	0
other species	10 ⁻¹⁵ ppm	10 ⁻¹⁵ ppm

The model also allows the specification of upper level smog concentrations from the previous day. For example it is suggested that the smog concentration observed at midday throughout the depth of the convective boundary layer on the pre-event day may be representative of the concentration observed at elevation during the event. We have not used this option for the SEQR study.